

# Compensatory Effects between CO<sub>2</sub>, Nitrogen Deposition, and Temperature in Terrestrial Biosphere Models without Nitrogen Compromise Projections of the Future Terrestrial Carbon Sink

Sian Kou-Giesbrecht<sup>1</sup> and Vivek Arora<sup>1</sup>

<sup>1</sup>Canadian Centre for Climate Modelling and Analysis

December 22, 2022

## Abstract

The strength of CO<sub>2</sub> fertilisation is a major uncertainty across terrestrial biosphere models (TBMs) and is suggested to be overestimated without a representation of nitrogen (N) limitation. Here, we compare TBM projections with and without coupled C and N cycling over alternative future scenarios (the Shared Socioeconomic Pathways) to examine how representing N cycling influences CO<sub>2</sub> fertilisation as well as the effects of a comprehensive group of physical and socioeconomic global change drivers. Because elevated N deposition and N mineralisation (driven by elevated temperature) have stimulated terrestrial C sequestration over the historical period, a TBM without N cycling must exaggerate the strength of CO<sub>2</sub> fertilisation to compensate for these unrepresented N processes and to reproduce the historical terrestrial C sink. As a result, it cannot reliably project the future terrestrial C sink, overestimating CO<sub>2</sub> fertilisation as CO<sub>2</sub> increases faster than N deposition and temperature in future scenarios.

## Hosted file

952565\_0\_art\_file\_10552565\_rn7nps.docx available at <https://authorea.com/users/568839/articles/614546-compensatory-effects-between-co2-nitrogen-deposition-and-temperature-in-terrestrial-biosphere-models-without-nitrogen-compromise-projections-of-the-future-terrestrial-carbon-sink>

## Hosted file

952565\_0\_supp\_10551971\_rn7dfv.docx available at <https://authorea.com/users/568839/articles/614546-compensatory-effects-between-co2-nitrogen-deposition-and-temperature-in-terrestrial-biosphere-models-without-nitrogen-compromise-projections-of-the-future-terrestrial-carbon-sink>

1        **Compensatory Effects between CO<sub>2</sub>, Nitrogen Deposition, and Temperature in**  
2        **Terrestrial Biosphere Models without Nitrogen Compromise Projections of the**  
3        **Future Terrestrial Carbon Sink**

4        **S. Kou-Giesbrecht<sup>1</sup> and V. K. Arora<sup>1</sup>**

5        <sup>1</sup>Canadian Centre for Climate Modelling and Analysis, Environment and Climate Change  
6        Canada

7        Corresponding author: Sian Kou-Giesbrecht (sian.kougiesbrecht@ec.gc.ca)

8        **Key Points:**

- 9        • Terrestrial biosphere models without N do not represent N deposition or mineralisation,  
10        which have stimulated terrestrial C sequestration
- 11        • Exaggerated CO<sub>2</sub> fertilisation compensates for N deposition and mineralisation in order  
12        to reproduce the historical terrestrial C sink
- 13        • Models cannot reliably project the future terrestrial C sink as CO<sub>2</sub> increases faster than N  
14        deposition and temperature in future scenarios

## 15 **Abstract**

16 The strength of CO<sub>2</sub> fertilisation is a major uncertainty across terrestrial biosphere models  
17 (TBMs) and is suggested to be overestimated without a representation of nitrogen (N) limitation.  
18 Here, we compare TBM projections with and without coupled C and N cycling over alternative  
19 future scenarios (the Shared Socioeconomic Pathways) to examine how representing N cycling  
20 influences CO<sub>2</sub> fertilisation as well as the effects of a comprehensive group of physical and  
21 socioeconomic global change drivers. Because elevated N deposition and N mineralisation  
22 (driven by elevated temperature) have stimulated terrestrial C sequestration over the historical  
23 period, a TBM without N cycling must exaggerate the strength of CO<sub>2</sub> fertilisation to  
24 compensate for these unrepresented N processes and to reproduce the historical terrestrial C sink.  
25 As a result, it cannot reliably project the future terrestrial C sink, overestimating CO<sub>2</sub> fertilisation  
26 as CO<sub>2</sub> increases faster than N deposition and temperature in future scenarios.

## 27 **Plain Language Summary**

28 Climate change models simulate the terrestrial carbon sink (in plant and soil biomass), which  
29 takes up a third of anthropogenic CO<sub>2</sub> emissions. However, these models have only recently  
30 included representations of nitrogen limitation of plant growth and thus its future influence is  
31 unclear. Here we compare a model with and without nitrogen cycling in comprehensive  
32 simulations of alternative future scenarios that depend on socioeconomic development over the  
33 21<sup>st</sup> century. We find that models without nitrogen cycling must exaggerate the influence of  
34 elevated atmospheric CO<sub>2</sub> on plant growth to compensate for unrepresented nitrogen cycling  
35 processes in order to correctly simulate the historical terrestrial carbon sink. Specifically, these  
36 models do not represent how elevated atmospheric nitrogen input (due to intensive agriculture  
37 and fossil fuel burning) and how elevated soil nitrogen (due to decomposition driven by rising  
38 temperature) have increased plant growth over the historical period. As a result, models without  
39 nitrogen cycling cannot reliably project the future terrestrial carbon sink because atmospheric  
40 CO<sub>2</sub> increases faster than both atmospheric nitrogen input and temperature. This will lead to an  
41 overestimation of the future terrestrial carbon sink with implications for future climate change  
42 projections and policy.

## 43 **1 Introduction**

44 The terrestrial C sink has increased over recent decades driven primarily by CO<sub>2</sub>  
45 fertilisation and it currently sequesters approximately 30% of anthropogenic CO<sub>2</sub> emissions  
46 (Friedlingstein et al., 2022; Walker et al., 2020). The persistence of the terrestrial C sink over the  
47 21<sup>st</sup> century is uncertain due to the combined influences of multiple global change drivers –  
48 rising CO<sub>2</sub> alongside rising temperature, varying precipitation, and land use change (Huntzinger  
49 et al., 2017). In particular, nitrogen (N) is an essential limiting nutrient (Elser et al., 2007a;  
50 Fernández-Martínez et al., 2014; LeBauer & Treseder, 2008; Wright et al., 2018) and constrains  
51 CO<sub>2</sub> fertilisation (Terrer et al., 2019; S. Wang et al., 2020). However, agricultural activities and  
52 fossil fuel use cause elevated N deposition which could alleviate N limitation (O’Sullivan et al.,  
53 2019; R. Wang et al., 2017). Elevated temperature drives soil organic matter decomposition  
54 which releases plant-available N, i.e., N mineralisation, and this could further alleviate N  
55 limitation (Liu et al., 2017). Consequently, the extent to which N limitation will constrain the  
56 future terrestrial C sink under this cast of interacting and intensifying global change drivers is  
57 unresolved.

58 Terrestrial biosphere models (TBMs) are the principal tool for simulating the terrestrial C  
59 sink and they serve as the land components in Earth System Models thereby informing climate  
60 change policy (IPCC, 2021). In TBMs, CO<sub>2</sub> fertilisation is suggested to be overestimated without  
61 a representation of N limitation: When TBM projections of the future terrestrial C sink under a  
62 high atmospheric CO<sub>2</sub> scenario were constrained with observations of N supply and N  
63 stoichiometry, terrestrial C sequestration was reduced by 20% (Wieder et al., 2015). However,  
64 this study only examined estimated constraints applied post hoc to simulations of TBMs without  
65 N cycling rather than including an explicit representation of N cycling in TBMs. More and more  
66 TBMs now include a representation of coupled C and N cycling (e.g., in the most recent Global  
67 Carbon Project 11 out of 17 TBMs included a representation of N cycling (Friedlingstein et al.,  
68 2022)) which allows for intercomparisons between TBMs with and without N cycling. These  
69 intercomparisons have found that TBMs with N cycling and TBMs without N cycling perform  
70 similarly in reproducing the historical terrestrial C sink (Seiler et al., 2022) but that their  
71 responses to different global change drivers acting over the historical period drivers diverge  
72 (Huntzinger et al., 2017). In particular, the strength of the CO<sub>2</sub> fertilisation effect over the  
73 historical period simulated by TBMs without N cycling was found to be over twice that  
74 simulated by TBMs with N cycling, N deposition increased terrestrial C sequestration by  
75 approximately 20% over the historical period as simulated by TBMs with N cycling (but was not  
76 represented in TBMs without N cycling) (O’Sullivan et al., 2019), and most TBMs with N  
77 cycling simulated overall terrestrial C sequestration in response to historical climate variation  
78 whereas most TBMs without N cycling simulated overall terrestrial C emissions in response to  
79 historical climate variation (Huntzinger et al., 2017). That both TBMs with and without N  
80 cycling can reproduce the historical terrestrial C sink despite simulating such divergent responses  
81 to individual global change drivers suggests that TBMs are tuned to reproduce the historical  
82 terrestrial C sink with unknown consequences for projections of the future terrestrial C sink.  
83 However, few studies have examined N cycling in plausible future scenarios that encompass all  
84 global change drivers, either examining historical simulations or focusing solely on CO<sub>2</sub> and/or  
85 N deposition (Goll et al., 2012; Smith et al., 2014; Sokolov et al., 2008; Thornton et al., 2009; Y.  
86 P. Wang et al., 2015; Zaehle et al., 2010).

87 Here we use the Canadian Land Surface Scheme including Biogeochemical Cycles  
88 (CLASSIC), the land component of the Canadian Earth System Model (CanESM5), to examine  
89 how representing coupled C and N cycling influences the response of terrestrial C sequestration  
90 to global change by comparing simulations of CLASSIC with and without coupled C and N  
91 cycling over the 21<sup>st</sup> century. By examining a single TBM with and without coupled C and N  
92 cycling, we can isolate the impact of explicitly representing coupled C and N cycling whereas  
93 intercomparisons across TBMs with and without N cycling do not account for other structural  
94 and parametric differences between TBMs that may obscure the effects of N cycling. CLASSIC  
95 represents both flexible vegetation C:N stoichiometry and the upregulation of symbiotic  
96 biological N fixation under N limitation (described and evaluated in Asaadi & Arora (2021) and  
97 Kou-Giesbrecht & Arora (2022)) thereby presenting an advanced representation of coupled C  
98 and N cycling in a TBM. We evaluate the role of N cycling under individual and combined  
99 contributions of a comprehensive group of physical and socioeconomic global change drivers:  
100 CO<sub>2</sub>, climate, N deposition, and land use change. We simulate the historical period and three  
101 alternative future scenarios that are based on the Shared Socioeconomic Pathways (SSP) (Riahi  
102 et al., 2017), which are the recent framework adopted by the Intergovernmental Panel on Climate  
103 Change (IPCC): SSP126 (“sustainability”) has low greenhouse gas emissions, SSP370 (“regional

104 rivalry”) has high greenhouse gas emissions, and SSP585 (“fossil-fueled development”) has very  
105 high greenhouse gas emissions.

## 106 **2 Materials and Methods**

### 107 2.1 CLASSIC overview

108 The Canadian Land Surface Scheme Including Biogeochemical Cycles (CLASSIC)  
109 (Melton et al., 2020; Seiler et al., 2021) is the land component in the family of the Canadian  
110 Earth System Models (CanESM) (Swart et al., 2019). CLASSIC simulates land-atmosphere  
111 fluxes of energy, momentum, water, carbon (C), and nitrogen (N). The physical component of  
112 CLASSIC simulates fluxes of energy, momentum, and water (Verseghy, 1991; Verseghy et al.,  
113 1993). The biogeochemical component of CLASSIC simulates the land-atmosphere exchange of  
114 C via photosynthesis, autotrophic respiration, heterotrophic respiration, land use change, and fire  
115 (Arora & Boer, 2005). For biogeochemical processes, vegetation is partitioned into nine plant  
116 functional types (PFTs): needleleaf evergreen trees, needleleaf deciduous trees, broadleaf  
117 evergreen trees, broadleaf cold deciduous trees, broadleaf drought deciduous trees, C<sub>3</sub> crops, C<sub>4</sub>  
118 crops, C<sub>3</sub> grasses, and C<sub>4</sub> grasses. CLASSIC prognostically simulates the amount of C in  
119 vegetation, litter, and soil organic matter pools for each PFT and over the bare soil fraction in  
120 each grid cell. CLASSIC simulates the land-atmosphere exchange of N via biological N fixation  
121 (free-living and symbiotic), specified N deposition and N fertiliser application, nitric oxide (NO)  
122 emissions, nitrous oxide (N<sub>2</sub>O) emissions, N<sub>2</sub> emissions, ammonia (NH<sub>3</sub>) volatilisation, N  
123 leaching, and land use change (Asaadi & Arora, 2021; Kou-Giesbrecht & Arora, 2022).  
124 CLASSIC prognostically simulates the amount of N in vegetation, litter, soil organic matter, and  
125 inorganic soil N (ammonium (NH<sub>4</sub><sup>+</sup>) and nitrate (NO<sub>3</sub><sup>-</sup>)) pools for each PFT and over the bare  
126 soil fraction in each grid cell. See Text S1 for a more detailed description of the physical and  
127 biogeochemical components of CLASSIC.

128 In CLASSIC-CN, photosynthesis is dependent on leaf N such that, when leaf N is low,  
129 photosynthesis is downregulated and, when leaf N is high, photosynthesis is upregulated (Asaadi  
130 & Arora, 2021; Kou-Giesbrecht & Arora, 2022). Additionally, vegetation exhibits a dynamic  
131 response to N limitation of plant growth. First, vegetation upregulates and downregulates  
132 symbiotic biological N fixation in response to weak N limitation and strong N limitation  
133 respectively (Kou-Giesbrecht & Arora, 2022). Second, vegetation has flexible stoichiometry and  
134 thus the vegetation C:N ratio responds to changing N limitation (Asaadi & Arora, 2021). In  
135 CLASSIC-C, N cycling is turned off and the downregulation of photosynthesis under increasing  
136 CO<sub>2</sub> is controlled by a parameter as explained in Arora et al. (2009). Briefly, this parameter,  
137 which ranges between 0 and 0.9, determines the rate of increase of photosynthesis with  
138 increasing CO<sub>2</sub>. When it is set to 0, photosynthesis does not increase with increasing CO<sub>2</sub>. When  
139 it is set to 0.9, photosynthesis increases with increasing CO<sub>2</sub> at an unconstrained rate. When it is  
140 set to 0.35, CLASSIC-C simulations estimate a global net atmosphere-land CO<sub>2</sub> flux that lies  
141 within uncertainty range of estimates from the Global Carbon Project (Friedlingstein et al.,  
142 2022).

### 143 2.2 Simulations

144 We use CLASSIC-C and CLASSIC-CN to simulate energy, momentum, water, C, and N  
145 fluxes at the global scale over the historical period (1851 – 2014) and over the future period  
146 (2015 – 2100) for three Shared Socioeconomic Pathways (SSPs; SSP126, SSP370, and SSP585).

147 For the historical period, we conducted simulations following the TRENDY protocol (for  
148 contributions to the Global Carbon Project (Friedlingstein et al., 2022)). We also conducted  
149 historical simulations following the Inter-Sectoral Impact Model Intercomparison Project  
150 (ISIMIP) protocol (Buchner & Reyer, 2021; Lange & Buchner, 2022) in order to launch future  
151 simulations following the ISIMIP protocol. Forcings are described in Table S1. For both the  
152 historical period and future period, we conducted simulations with all global change drivers  
153 acting concurrently as well as four separate simulation experiments to disentangle the  
154 contributions of CO<sub>2</sub>, climate, N deposition, and land use change (which includes changes to  
155 both crop area and to N fertilisation of crops) to the global net atmosphere-land CO<sub>2</sub> flux. We did  
156 not isolate the influence of population density and CH<sub>4</sub> because these forcings regulate fire C  
157 emissions and soil CH<sub>4</sub> fluxes respectively, which have minimal influence on the global net  
158 atmosphere-land CO<sub>2</sub> flux in comparison to CO<sub>2</sub>, climate, land use change, and N deposition.  
159 Simulations are described in detail in Text S2 and in Tables S2 and S3.

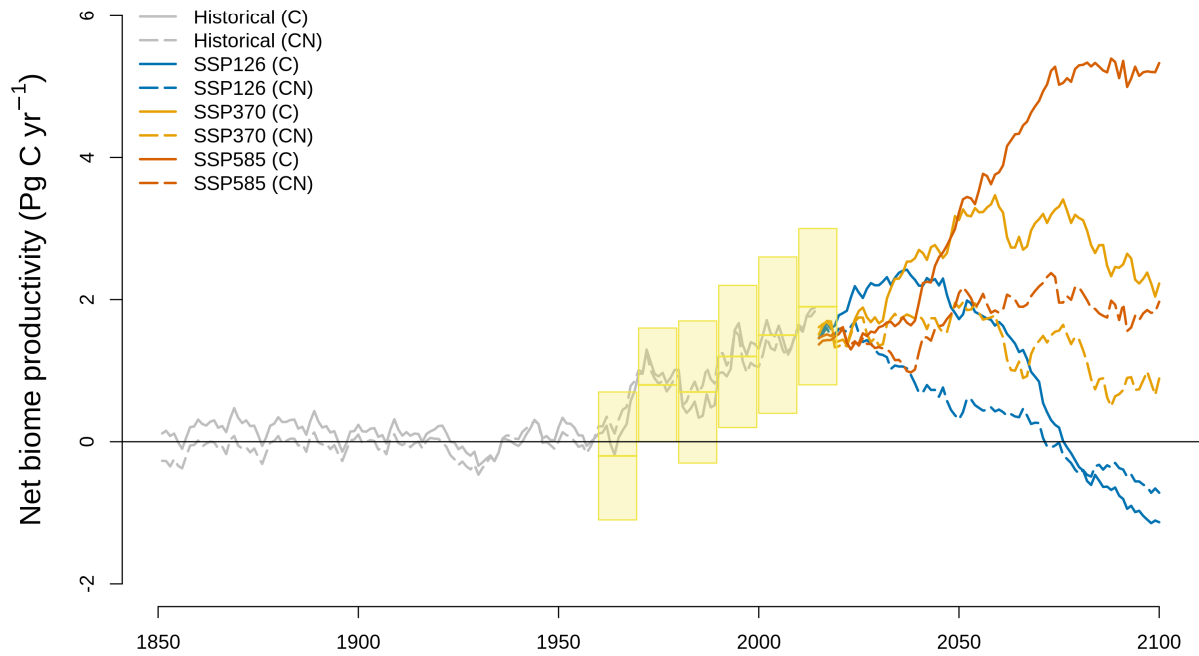
160 Over the historical period, we compared the global net atmosphere-land CO<sub>2</sub> flux  
161 simulated by CLASSIC-C and CLASSIC-CN to estimates from the Global Carbon Project  
162 (Friedlingstein et al., 2022). CLASSIC-C and CLASSIC-CN simulations over the historical  
163 period have been validated previously in other studies (Asaadi & Arora, 2021; Kou-Giesbrecht &  
164 Arora, 2022; Melton et al., 2020; Seiler et al., 2021).

## 165 **3 Results**

### 166 3.1 Historical net biome productivity

167 The net biome productivity (NBP) is the global net atmosphere-land CO<sub>2</sub> flux and  
168 quantifies the terrestrial C sink (or source). NBP ultimately determines changes in atmospheric  
169 CO<sub>2</sub> concentration (together with the global net atmosphere-ocean CO<sub>2</sub> flux and fossil fuel CO<sub>2</sub>  
170 emissions). Figure 1 shows simulated NBP over the historical period as well as NBP over the  
171 21<sup>st</sup> century under three SSPs.

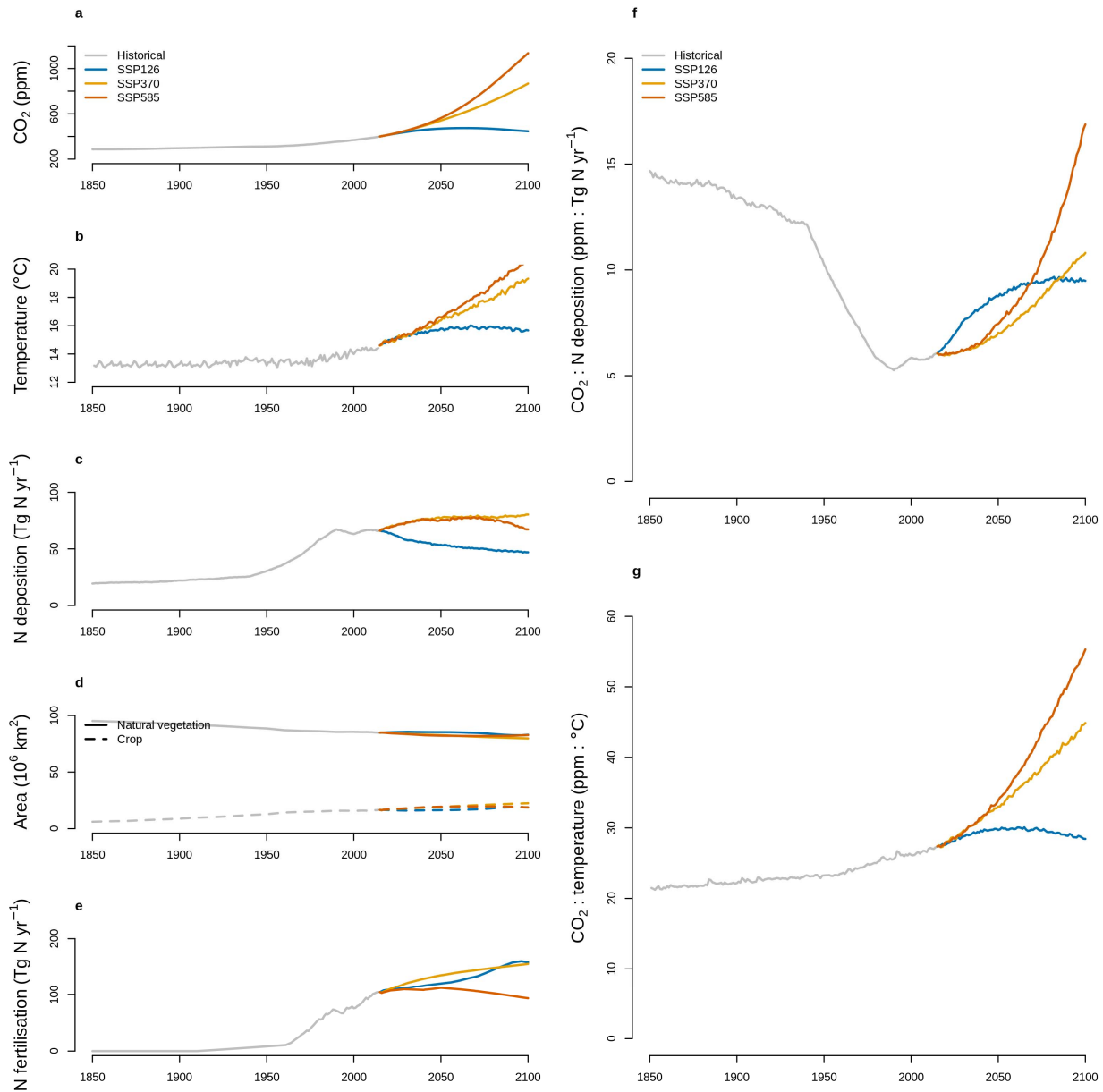
172 **Figure 1.** Net biome productivity (NBP) over the historical period and for future scenarios  
 173 simulated by CLASSIC-C (which does not represent N cycling, indicated by solid lines) and  
 174 CLASSIC-CN (which represents coupled C and N cycling, indicated by dashed lines). Historical  
 175 simulations follow the TRENDY protocol (1851 – 2014). Future simulations for SSP126  
 176 (“sustainability”), SSP370 (“regional rivalry”), and SSP585 (“fossil-fueled development”) follow  
 177 the ISIMIP protocol (2015 – 2100). Yellow boxes indicate the NBP range from other models in  
 178 the Global Carbon Project.



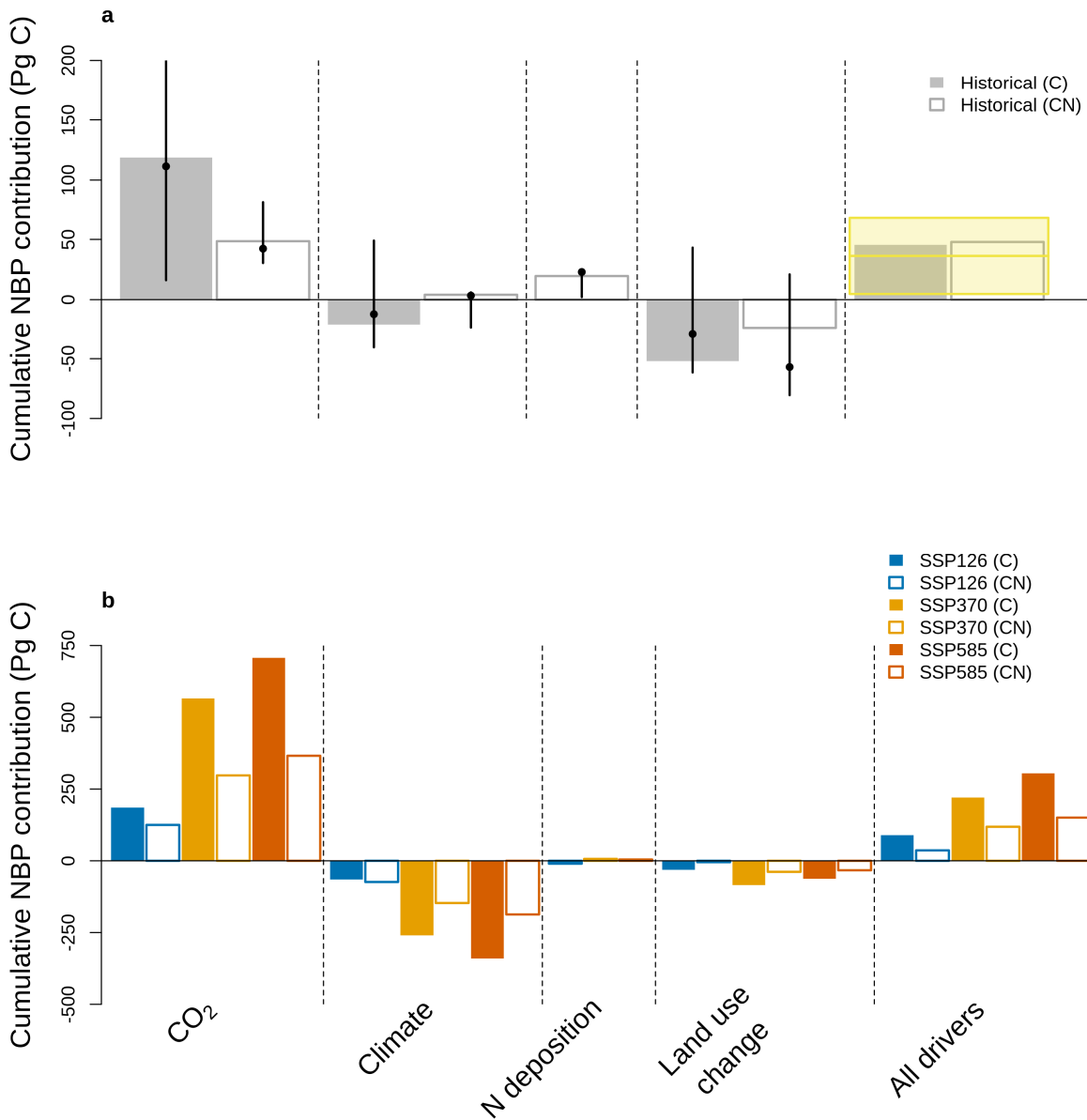
180 NBP simulated by CLASSIC-C (which does not represent N cycling) and CLASSIC-CN  
181 (which represents coupled C and N cycling) are similar over the historical period (Figure 1).  
182 Positive NBP values since the 1960s indicate a terrestrial C sink over the historical period.  
183 CLASSIC-C and CLASSIC-CN simulate a NBP of  $1.3 \text{ Pg C yr}^{-1}$  and  $1.2 \text{ Pg C yr}^{-1}$  (averaged  
184 over 2000 – 2010), respectively. Both these estimates lie within the uncertainty range of NBP  
185 estimates from the Global Carbon Project ( $1.3 \pm 0.6 \text{ Pg C yr}^{-1}$  from TBMs and  $1.0\text{--}1.8 \text{ Pg C yr}^{-1}$   
186 from atmospheric inversions; averaged over 2000 – 2010).

187 NBP is driven by contributions from a comprehensive group of physical and  
188 socioeconomic global change drivers:  $\text{CO}_2$  (Figure 2a), climate (Figure 2b,c), N deposition  
189 (Figure 2d), and land use change (which includes changes to both crop area and N fertilisation of  
190 crops; Figure 2e,f). Despite both CLASSIC-C and CLASSIC-CN exhibiting a similar NBP when  
191 all global change drivers act concurrently that compares well with NBP estimates from the  
192 Global Carbon Project (Figure 1), the cumulative NBP contributions over the historical period  
193 from each global change driver differ between CLASSIC-C and CLASSIC-CN (Figure 3a). In  
194 particular, CLASSIC-C exhibits a significantly stronger NBP increase driven by  $\text{CO}_2$  than  
195 CLASSIC-CN over the historical period (Figure 3a). Because CLASSIC-C does not represent N  
196 cycling, it does not represent the effects of N deposition, N mineralisation, or N fertilisation of  
197 crops. In CLASSIC-CN, elevated N deposition relieves N limitation and stimulates NBP over the  
198 historical period. In CLASSIC-CN, elevated N mineralisation (which is driven by elevated  
199 temperature (Asaadi & Arora, 2021)) also relieves N limitation and stimulates NBP over the  
200 historical period. In CLASSIC-C, varying climate over the historical period decreases NBP due  
201 to increasing heterotrophic respiration driven by elevated temperature and thus the contribution  
202 of climate to cumulative NBP over the historical period is negative. In CLASSIC-CN, this NBP  
203 decrease is offset by N mineralisation and the contribution of climate to cumulative NBP over  
204 the historical period is positive. Finally, in CLASSIC-CN, elevated N fertilisation of crops also  
205 relieves N limitation and stimulates NBP over the historical period. The contribution of land use  
206 change to cumulative NBP over the historical period is negative for both CLASSIC-CN and  
207 CLASSIC-C due to  $\text{CO}_2$  emissions associated with the conversion of natural vegetation to crops  
208 but this NBP decrease is weaker for CLASSIC-CN than for CLASSIC-C because it is offset by  
209 stimulated NBP due to N fertilisation. In CLASSIC-CN, the contributions of both N deposition  
210 and climate (i.e., N mineralisation) to cumulative NBP over the historical period were stronger at  
211 higher latitudes, which are often N-limited (Hedin et al., 2009) (Figure S1).

212 **Figure 2.** Global change drivers over the historical period (1851 – 2014) and for future scenarios  
 213 (2015 – 2100) for SSP126 (“sustainability”), SSP370 (“regional rivalry”), and SSP585 (“fossil-  
 214 fueled development”). a. CO<sub>2</sub>. b. Temperature (globally averaged over land excluding Greenland  
 215 and Antarctica). c. N deposition. d. Land cover. e. N fertilisation of crops. f. Ratio of CO<sub>2</sub> to N  
 216 deposition. g. Ratio of CO<sub>2</sub> to temperature. Historical forcings are from the TRENDY protocol.  
 217 Future forcings for SSP126 (“sustainability”), SSP370 (“regional rivalry”), and SSP585 (“fossil-  
 218 fueled development”) are from the ISIMIP protocol. In f, decreasing CO<sub>2</sub> : N deposition ratio  
 219 over the historical period indicates that N deposition is increasing faster than CO<sub>2</sub>, whereas  
 220 increasing CO<sub>2</sub> : N deposition ratio in the future scenarios indicates that CO<sub>2</sub> is increasing faster  
 221 than N deposition. In g, increasing CO<sub>2</sub> : temperature ratio is due to the logarithmic relationship  
 222 between temperature and CO<sub>2</sub> (Shine et al., 1990).



224 **Figure 3.** Contributions of CO<sub>2</sub>, climate, N deposition, and land use change (includes both  
 225 changes to both crop area and to N fertilisation of crops) to cumulative net biome productivity  
 226 (NBP) over the historical period (1851 – 2014; a) and for future scenarios (2015 – 2100; b)  
 227 simulated by CLASSIC-C (which does not represent N cycling) and CLASSIC-CN (which  
 228 represents coupled C and N cycling). Historical simulations follow the TRENDY protocol.  
 229 Future simulations for SSP126 (“sustainability”), SSP370 (“regional rivalry”), and SSP585  
 230 (“fossil-fueled development”) follow the ISIMIP protocol. The yellow box indicates the range  
 231 from other models in the Global Carbon Project. Black dots and lines indicate the median and  
 232 95% confidence interval of other models with coupled C and N cycling from Huntzinger et al.  
 233 (2017). Figure S2 shows the time series of the contribution of each global change driver to  
 234 cumulative NBP.



236 Overall, because CLASSIC-C and other similar TBMs that do not represent N cycling  
 237 (Huntzinger et al., 2017) are unable to represent the stimulation of terrestrial C sequestration by  
 238 N deposition, N mineralisation, or N fertilisation of crops over the historical period. Therefore,  
 239 the stimulation of terrestrial C sequestration by elevated CO<sub>2</sub> over the historical period must be  
 240 exaggerated to compensate for these unrepresented N processes in order to reproduce the  
 241 historical terrestrial C sink. Essentially, in TBMs that do not represent N cycling, the sensitivity  
 242 of terrestrial photosynthesis to CO<sub>2</sub> is calibrated to reproduce the terrestrial C sink over the  
 243 historical period (Arora et al., 2009; Delire et al., 2020; Krinner et al., 2005). This introduces  
 244 these compensatory effects and overestimates the CO<sub>2</sub> effect by design. We now explore the  
 245 consequences of these compensatory effects in projections of the future terrestrial C sink.

## 246 2.2 Future net biome productivity

247 Despite the agreement between NBP simulated by CLASSIC-C and CLASSIC-CN over  
 248 the historical period and their agreement with NBP estimates from the Global Carbon Project,  
 249 there are major differences between NBP projected by CLASSIC-C and CLASSIC-CN over the  
 250 21<sup>st</sup> century, especially in future scenarios characterised by high atmospheric CO<sub>2</sub>. At the end of  
 251 the 21<sup>st</sup> century, projections of NBP by CLASSIC-C and CLASSIC-CN differ by 0.5 Pg C yr<sup>-1</sup>  
 252 for SSP126, by 1.4 Pg C yr<sup>-1</sup> for SSP370, and by 3.3 Pg C yr<sup>-1</sup> for SSP585 (averaged over 2090 –  
 253 2100; Figure 1).

254 In SSP126 (“sustainability”), CO<sub>2</sub> and temperature stabilise then decrease after 2050  
 255 while N deposition decreases (Figure 2). Thus, CLASSIC-C and CLASSIC-CN project  
 256 decreasing NBP over the 21<sup>st</sup> century due to the contributions of climate and land use change  
 257 (Figures 1 and 3b). Note that, in SSP126, the terrestrial C sink transitions to a terrestrial C source  
 258 because photosynthesis decreases due to decreasing CO<sub>2</sub> while heterotrophic respiration persists  
 259 given its longer timescale. In both SSP370 (“regional rivalry”) and SSP585 (“fossil-fueled  
 260 development”), CO<sub>2</sub>, temperature, and N deposition increase (Figure 2). CLASSIC-C and  
 261 CLASSIC-CN project increasing NBP for SSP370 over the 21<sup>st</sup> century primarily due to  
 262 increasing CO<sub>2</sub> (Figures 1 and 3b).

263 Under SSP370 (“regional rivalry”), although CO<sub>2</sub>, temperature, and N deposition  
 264 increase simultaneously as in the historical period, CO<sub>2</sub> increases at a faster rate than N  
 265 deposition (Figure 2f) and temperature (Figure 2g). Under SSP585 (“fossil-fueled  
 266 development”), CO<sub>2</sub> and temperature increase whereas N deposition peaks then decreases as  
 267 opposed to the historical period over which CO<sub>2</sub>, temperature, and N deposition all increase  
 268 simultaneously (Figure 2fg). Similar to SSP370, CO<sub>2</sub> increases at a faster rate than temperature  
 269 in SSP585 (Figure 2g). Over the historical period, the contribution of N deposition to cumulative  
 270 NBP was 19.6 Pg C (20% of 96.5 Pg C) whereas the contribution of CO<sub>2</sub> to cumulative NBP was  
 271 48.5 Pg C (51% of 96.5 Pg C) for CLASSIC-CN and 118.6 Pg C (62% of 191.8 Pg C) for  
 272 CLASSIC-C (Figure 3b and Table S4). The contribution of N deposition relative to that of CO<sub>2</sub>  
 273 to cumulative NBP is much weaker in future scenarios than over the historical period. For  
 274 SSP370 and SSP585, the contributions of N deposition to cumulative NBP were only 6.6 Pg C  
 275 (1% of 489.6 Pg C) and 4.4 Pg C (1% of 590.2 Pg C), respectively. In comparison, the  
 276 contributions of CO<sub>2</sub> to cumulative NBP were 297.5 Pg C (60% of 489.6 Pg C) in SSP370 and  
 277 365.9 Pg C (61% of 590.2 Pg C) in SSP585 for CLASSIC-CN and were 565.2 Pg C (62% of  
 278 910.6 Pg C) in SSP370 and 707.1 Pg C (63% of 1109.8 Pg C) in SSP585 for CLASSIC-C  
 279 (Figure 3b and Table S4).

280 Therefore, for SSP370, CLASSIC-CN projects a terrestrial C sink that is  $1.4 \text{ Pg C yr}^{-1}$   
281 lower (58% lower) than that projected by CLASSIC-C at the end of the 21<sup>st</sup> century (Figure 1).  
282 For SSP585, the discrepancy between CLASSIC-C and CLASSIC-CN is substantial: CLASSIC-  
283 CN projects a terrestrial C sink that is  $3.3 \text{ Pg C yr}^{-1}$  lower (64% lower) than that projected by  
284 CLASSIC-C at the end of the 21<sup>st</sup> century (Figure 1).

#### 285 4 Discussion

286 Of critical importance, as we show here, is that while a TBM that does not represent  
287 coupled C and N cycling can reproduce the historical terrestrial C sink, it cannot reliably project  
288 the future terrestrial C sink. This is because, in a TBM that does not represent coupled C and N  
289 cycling, calibrating the sensitivity of terrestrial photosynthesis to  $\text{CO}_2$  to reproduce the historical  
290 terrestrial C sink in the absence of N cycling introduces compensatory effects: the stimulation of  
291 terrestrial C sequestration by elevated  $\text{CO}_2$  over the historical period (i.e., the  $\text{CO}_2$  fertilisation  
292 effect) must be exaggerated to compensate for the absence of N cycling, i.e., the stimulation of  
293 terrestrial C sequestration by elevated N deposition and elevated N mineralisation (driven by  
294 elevated temperature) over the historical period. The result of these compensatory effects is that  
295 a TBM that does not represent coupled C and N cycling but reproduces the historical terrestrial C  
296 sink correctly cannot reliably project the future terrestrial C sink as global change drivers follow  
297 divergent trajectories and occur in unprecedented combinations. Specifically, it will overestimate  
298 the  $\text{CO}_2$  fertilisation effect as  $\text{CO}_2$  increases faster than N deposition (which also decreases in  
299 some future scenarios) and temperature. This is supported by our simulations of the terrestrial C  
300 sink in future scenarios characterised by high atmospheric  $\text{CO}_2$ : the TBM used here with coupled  
301 C and N cycling projects a global net atmosphere-land  $\text{CO}_2$  flux that is between  $1.4$  and  $3.3 \text{ Pg C}$   
302  $\text{yr}^{-1}$  lower (58% to 64% lower) than that projected by the TBM used here without coupled C and  
303 N cycling at the end of the 21<sup>st</sup> century.

304 Numerous lines of evidence have suggested the importance of N limitation in  
305 constraining  $\text{CO}_2$  fertilisation, including meta-analyses of elevated  $\text{CO}_2$  experiments (Terrer et  
306 al., 2019) and temporal analyses of satellite-based estimates of terrestrial photosynthesis paired  
307 with foliar N observations (S. Wang et al., 2020). Consistent with these studies, we show that  
308 explicitly representing N limitation in a TBM reduces the  $\text{CO}_2$  fertilisation effect. Additionally, it  
309 has been proposed that the dynamic response of vegetation to N limitation, whereby vegetation  
310 invests C in N uptake strategies (such as symbiotic biological N fixation (Vitousek et al., 2013),  
311 mycorrhizae (Phillips et al., 2013), rhizosphere priming (Cheng et al., 2014; Finzi et al., 2015),  
312 and increasing root:shoot ratio (Poorter et al., 2012; Z. Wang & Wang, 2021)) and/or N retention  
313 strategies (such as increasing N resorption (Reed et al., 2012; Z. Wang & Wang, 2021) and  
314 increasing C:N ratios (Elser et al., 2010; Sistla & Schimel, 2012; Z. Wang & Wang, 2021)) could  
315 allow vegetation to overcome N limitation. The TBM used here includes an advanced  
316 representation of symbiotic biological N fixation (Kou-Giesbrecht & Arora, 2022) as well as a  
317 representation of flexible C:N stoichiometry (Asaadi & Arora, 2021), suggesting that the  
318 dynamic response of vegetation to N limitation (via these two strategies) is insufficient to relieve  
319 N limitation of  $\text{CO}_2$  fertilisation. Finally, phosphorus (P) could also be imperative in constraining  
320  $\text{CO}_2$  fertilisation, especially in tropical regions (Elser et al., 2007b). Additional compensatory  
321 effects could exist in TBMs to compensate for the absence of P cycling and require further  
322 analysis.

323 The overestimation of the CO<sub>2</sub> fertilisation effect by TBMs without coupled C and N  
324 cycling extends to climate change projections by Earth System Models. CLASSIC serves as the  
325 land component of the Canadian Earth System Model (CanESM5) (Swart et al., 2019), which  
326 contributed to the sixth phase of the Coupled Model Intercomparison Project (CMIP6) (Eyring et  
327 al., 2016). In CanESM5, which includes the older version of CLASSIC that does not represent  
328 coupled C and N cycling, the projected global net atmosphere-land CO<sub>2</sub> flux reaches a staggering  
329 12.0 Pg C yr<sup>-1</sup> at the end of the 21<sup>st</sup> century for the future scenario with the highest CO<sub>2</sub>  
330 (SSP585). This estimate was the highest among participating Earth System Models in CMIP6,  
331 despite CanESM5's ability to reproduce several aspects of the historical global C budget (Arora  
332 & Scinocca, 2016), and was closely followed by estimates from two other Earth System Models  
333 without a representation of coupled terrestrial C and N cycling (Arora et al., 2020; Koven et al.,  
334 2022).

## 335 **5 Conclusions**

336 Our analyses show that reproduction of the historical terrestrial C sink, which is achieved  
337 successfully by most TBMs (Friedlingstein et al., 2022), cannot be considered an indicator for  
338 the reliability of their projections of the future terrestrial C sink. Our findings show that a TBM  
339 that does not represent coupled C and N cycling cannot represent the combined influences of  
340 multiple global change drivers, overestimating CO<sub>2</sub> fertilisation as CO<sub>2</sub> increases faster than N  
341 deposition and temperature over the 21<sup>st</sup> century. Scaling fundamental ecological understanding  
342 of C and N interactions to the global scale through the explicit representation of physical and  
343 biological processes rather than calibration to reproduce the historical terrestrial C sink is key for  
344 reliably projecting the future terrestrial C sink under global change with TBMs and ultimately  
345 climate change with Earth System Models.

346 **Acknowledgments**

347 The authors would like to thank the input from the CLASSIC team (Mike Brady, Ed Chan,  
348 Salvatore Curasi, Joe Melton, Gesa Meyer, Christian Seiler, and Libo Wang).

349

350 **Open Research**

351 The source code for CLASSIC is available on the CLASSIC community Zenodo page  
352 (<https://zenodo.org/record/6499554#.YmrLy-3MKUI>).

353

354 **References**

- 355 Arora, V. K., & Boer, G. J. (2005). A parameterization of leaf phenology for the terrestrial ecosystem component of  
356 climate models. *Global Change Biology*, *11*(1), 39–59. <https://doi.org/10.1111/j.1365-2486.2004.00890.x>
- 357 Arora, V. K., & Scinocca, J. F. (2016). Constraining the strength of the terrestrial CO<sub>2</sub> fertilization effect in the  
358 Canadian Earth system model version 4.2 (CanESM4.2). *Geoscientific Model Development*, *9*(7), 2357–  
359 2376. <https://doi.org/10.5194/gmd-9-2357-2016>
- 360 Arora, V. K., Boer, G. J., Christian, J. R., Curry, C. L., Denman, K. L., Zahariev, K., et al. (2009). The effect of  
361 terrestrial photosynthesis down regulation on the twentieth-century carbon budget simulated with the  
362 CCCma Earth System Model. *Journal of Climate*, *22*(22), 6066–6088.  
363 <https://doi.org/10.1175/2009JCLI3037.1>
- 364 Arora, V. K., Katavouta, A., Williams, R. G., Jones, C. D., Brovkin, V., Friedlingstein, P., et al. (2020). Carbon–  
365 concentration and carbon–climate feedbacks in CMIP6 models and their comparison to CMIP5 models.  
366 *Biogeosciences*, *17*(16), 4173–4222. <https://doi.org/10.5194/bg-17-4173-2020>
- 367 Asaadi, A., & Arora, V. K. (2021). Implementation of nitrogen cycle in the CLASSIC land model. *Biogeosciences*,  
368 *18*(2), 669–706. <https://doi.org/10.5194/bg-18-669-2021>
- 369 Buchner, M., & Reyer, C. (2021). ISIMIP3b bias-adjusted atmospheric climate input data (Version 1.1). ISIMIP  
370 Repository. <https://doi.org/10.48364/ISIMIP.842396.1>

- 371 Cheng, W., Parton, W. J., Gonzalez-Meler, M. A., Phillips, R., Asao, S., McNickle, G. G., et al. (2014). Synthesis  
372 and modeling perspectives of rhizosphere priming. *New Phytologist*, *201*(1), 31–44.  
373 <https://doi.org/10.1111/nph.12440>
- 374 Delire, C., Séférian, R., Decharme, B., Alkama, R., Calvet, J., Carrer, D., et al. (2020). The global land carbon cycle  
375 simulated with ISBA-CTRIP: Improvements over the last decade. *Journal of Advances in Modeling Earth*  
376 *Systems*, *12*(9), e2019MS001886.
- 377 Elser, J. J., Bracken, M. E. S., Cleland, E. E., Gruner, D. S., Harpole, W. S., Hillebrand, H., et al. (2007a). Global  
378 analysis of nitrogen and phosphorus limitation of primary producers in freshwater, marine and terrestrial  
379 ecosystems. *Ecology Letters*, *10*(12), 1135–1142. <https://doi.org/10.1111/j.1461-0248.2007.01113.x>
- 380 Elser, J. J., Bracken, M. E. S., Cleland, E. E., Gruner, D. S., Harpole, W. S., Hillebrand, H., et al. (2007b). Global  
381 analysis of nitrogen and phosphorus limitation of primary producers in freshwater, marine and terrestrial  
382 ecosystems. *Ecology Letters*, *10*(12), 1135–1142. <https://doi.org/10.1111/j.1461-0248.2007.01113.x>
- 383 Elser, J. J., Fagan, W. F., Kerkhoff, A. J., Swenson, N. G., & Enquist, B. J. (2010). Biological stoichiometry of plant  
384 production: Metabolism, scaling and ecological response to global change. *New Phytologist*, *186*(3), 593–  
385 608. <https://doi.org/10.1111/j.1469-8137.2010.03214.x>
- 386 Eyring, V., Bony, S., Meehl, G. A., Senior, C. A., Stevens, B., Stouffer, R. J., & Taylor, K. E. (2016). Overview of  
387 the Coupled Model Intercomparison Project Phase 6 (CMIP6) experimental design and organization.  
388 *Geoscientific Model Development*, *9*(5), 1937–1958. <https://doi.org/10.5194/gmd-9-1937-2016>
- 389 Fernández-Martínez, M., Vicca, S., Janssens, I. A., Sardans, J., Luysaert, S., Campioli, M., et al. (2014). Nutrient  
390 availability as the key regulator of global forest carbon balance. *Nature Climate Change*, *4*(6), 471–476.  
391 <https://doi.org/10.1038/nclimate2177>
- 392 Finzi, A. C., Abramoff, R. Z., Spiller, K. S., Brzostek, E. R., Darby, B. A., Kramer, M. A., & Phillips, R. P. (2015).  
393 Rhizosphere processes are quantitatively important components of terrestrial carbon and nutrient cycles.  
394 *Global Change Biology*, *21*(5), 2082–2094. <https://doi.org/10.1111/gcb.12816>
- 395 Friedlingstein, P., Jones, M. W., O’Sullivan, M., Andrew, R. M., Bakker, D. C. E., Hauck, J., et al. (2022). Global  
396 Carbon Budget 2021. *Earth Syst. Sci. Data*, *14*(4), 1917–2005. <https://doi.org/10.5194/essd-14-1917-2022>

- 397 Goll, D. S., Brovkin, V., Parida, B. R., Reick, C. H., Kattge, J., Reich, P. B., et al. (2012). Nutrient limitation  
398 reduces land carbon uptake in simulations with a model of combined carbon, nitrogen and phosphorus  
399 cycling. *Biogeosciences*, *9*(9), 3547–3569. <https://doi.org/10.5194/bg-9-3547-2012>
- 400 Hedin, L. O., Brookshire, E. N. J., Menge, D. N. L., & Barron, A. R. (2009). The Nitrogen Paradox in Tropical  
401 Forest Ecosystems. *Annual Review of Ecology, Evolution, and Systematics*, *40*(1), 613–635.  
402 <https://doi.org/10.1146/annurev.ecolsys.37.091305.110246>
- 403 Huntzinger, D. N., Michalak, A. M., Schwalm, C., Ciais, P., King, A. W., Fang, Y., et al. (2017). Uncertainty in the  
404 response of terrestrial carbon sink to environmental drivers undermines carbon-climate feedback  
405 predictions. *Scientific Reports*, *7*(1), 1–8. <https://doi.org/10.1038/s41598-017-03818-2>
- 406 IPCC. (2021). *Summary for Policymakers* (Climate Change 2021: The Physical Science Basis. Contribution of  
407 Working Group I to the Sixth Assessment Report of the Intergovernmental Panel on Climate Change No.  
408 9789291691586). <https://doi.org/10.1260/095830507781076194>
- 409 Kou-Giesbrecht, S., & Arora, V. K. (2022). Representing the Dynamic Response of Vegetation to Nitrogen  
410 Limitation via Biological Nitrogen Fixation in the CLASSIC Land Model. *Global Biogeochemical Cycles*,  
411 *36*(6), e2022GB007341. <https://doi.org/10.1029/2022GB007341>
- 412 Koven, C. D., Arora, V. K., Cadule, P., Fisher, R. A., Jones, C. D., Lawrence, D. M., et al. (2022). Multi-century  
413 dynamics of the climate and carbon cycle under both high and net negative emissions scenarios. *Earth*  
414 *System Dynamics*, *13*(2), 885–909. <https://doi.org/10.5194/esd-13-885-2022>
- 415 Krinner, G., Viovy, N., de Noblet-Ducoudré, N., Ogée, J., Polcher, J., Friedlingstein, P., et al. (2005). A dynamic  
416 global vegetation model for studies of the coupled atmosphere-biosphere system. *Global Biogeochemical*  
417 *Cycles*, *19*(1).
- 418 Lange, S., & Buchner, M. (2022). ISIMIP3b atmospheric composition input data (Version 1.1). ISIMIP Repository.  
419 <https://doi.org/10.48364/ISIMIP.482153.1>
- 420 LeBauer, D. S., & Treseder, K. K. (2008). Nitrogen Limitation of Net Primary Productivity in Terrestrial  
421 Ecosystems is Globally Distributed. *Ecology*, *89*(2), 371–379. <https://doi.org/10.1016/j.agee.2013.04.020>
- 422 Liu, Y., Wang, C., He, N., Wen, X., Gao, Y., Li, S., et al. (2017). A global synthesis of the rate and temperature  
423 sensitivity of soil nitrogen mineralization: latitudinal patterns and mechanisms. *Global Change Biology*,  
424 *23*(1), 455–464. <https://doi.org/10.1111/gcb.13372>

- 425 Melton, J. R., Arora, V. K., Wisernig-Cojoc, E., Seiler, C., Fortier, M., Chan, E., & Teckentrup, L. (2020).  
426 CLASSIC v1.0: The open-source community successor to the Canadian Land Surface Scheme (CLASS)  
427 and the Canadian Terrestrial Ecosystem Model (CTEM)-Part 1: Model framework and site-level  
428 performance. *Geoscientific Model Development*, 13(6), 2825–2850. [https://doi.org/10.5194/gmd-13-2825-](https://doi.org/10.5194/gmd-13-2825-2020)  
429 2020
- 430 O’Sullivan, M., Spracklen, D. V., Batterman, S. A., Arnold, S. R., Gloor, M., & Buermann, W. (2019). Have  
431 Synergies Between Nitrogen Deposition and Atmospheric CO<sub>2</sub> Driven the Recent Enhancement of the  
432 Terrestrial Carbon Sink? *Global Biogeochemical Cycles*, 33(2), 163–180.  
433 <https://doi.org/10.1029/2018GB005922>
- 434 Phillips, R. P., Brzostek, E., & Midgley, M. G. (2013). The mycorrhizal-associated nutrient economy: A new  
435 framework for predicting carbon-nutrient couplings in temperate forests. *New Phytologist*, 199(1), 41–51.  
436 <https://doi.org/10.1111/nph.12221>
- 437 Poorter, H., Niklas, K. J., Reich, P. B., Oleksyn, J., Poot, P., & Mommer, L. (2012). Biomass allocation to leaves,  
438 stems and roots: Meta-analyses of interspecific variation and environmental control. *New Phytologist*,  
439 193(1), 30–50. <https://doi.org/10.1111/j.1469-8137.2011.03952.x>
- 440 Reed, S. C., Townsend, A. R., Davidson, E. A., & Cleveland, C. C. (2012). Stoichiometric patterns in foliar nutrient  
441 resorption across multiple scales. *New Phytologist*, 196(1), 173–180. [https://doi.org/10.1111/j.1469-](https://doi.org/10.1111/j.1469-8137.2012.04249.x)  
442 8137.2012.04249.x
- 443 Riahi, K., van Vuuren, D. P., Kriegler, E., Edmonds, J., O’Neill, B. C., Fujimori, S., et al. (2017). The Shared  
444 Socioeconomic Pathways and their energy, land use, and greenhouse gas emissions implications: An  
445 overview. *Global Environmental Change*, 42, 153–168. <https://doi.org/10.1016/j.gloenvcha.2016.05.009>
- 446 Seiler, C., Melton, J., Arora, V., & Wang, L. (2021). CLASSIC v1.0: the open-source community successor to the  
447 Canadian Land Surface Scheme (CLASS) and the Canadian Terrestrial Ecosystem Model (CTEM) – Part  
448 2: Global Benchmarking. *Geoscientific Model Development*, 14(5), 2371–2417.  
449 <https://doi.org/10.5194/gmd-2020-294>
- 450 Seiler, C., Melton, J. R., Arora, V. K., Sitch, S., Friedlingstein, P., Anthoni, P., et al. (2022). Are Terrestrial  
451 Biosphere Models Fit for Simulating the Global Land Carbon Sink? *Journal of Advances in Modeling*  
452 *Earth Systems*, 14(5), e2021MS002946. <https://doi.org/10.1029/2021MS002946>

- 453 Shine, K. P., Derwent, R. G., Wuebbles, D. J., & Morcrette, J. J. (1990). *Radiative forcing of climate. Climate*  
454 *change: The IPCC scientific assessment*. (pp. 41–68).
- 455 Sistla, S. A., & Schimel, J. P. (2012). Stoichiometric flexibility as a regulator of carbon and nutrient cycling in  
456 terrestrial ecosystems under change. *New Phytologist*, *196*(1), 68–78. [https://doi.org/10.1111/j.1469-](https://doi.org/10.1111/j.1469-8137.2012.04234.x)  
457 [8137.2012.04234.x](https://doi.org/10.1111/j.1469-8137.2012.04234.x)
- 458 Smith, B., Wårlind, D., Arneth, A., Hickler, T., Leadley, P., Siltberg, J., & Zaehle, S. (2014). Implications of  
459 incorporating N cycling and N limitations on primary production in an individual-based dynamic  
460 vegetation model. *Biogeosciences*, *11*(7), 2027–2054. <https://doi.org/10.5194/bg-11-2027-2014>
- 461 Sokolov, A. P., Kicklighter, D. W., Melillo, J. M., Felzer, B. S., Schlosser, C. A., & Cronin, T. W. (2008).  
462 Consequences of considering carbon–nitrogen interactions on the feedbacks between climate and the  
463 terrestrial carbon cycle. *Journal of Climate*, *21*(15), 3776–3796.
- 464 Swart, N. C., Cole, J. N. S., Kharin, V. V., Lazare, M., Scinocca, J. F., Gillett, N. P., et al. (2019). The Canadian  
465 Earth System Model version 5 (CanESM5.0.3). *Geoscientific Model Development*, *12*(11), 4823–4873.  
466 <https://doi.org/10.5194/gmd-12-4823-2019>
- 467 Terrer, C., Prentice, I., Jackson, R., Keenan, T., Kaiser, C., Vicca, S., et al. (2019). Nitrogen and phosphorus  
468 constrain the CO<sub>2</sub> fertilization of global plant biomass. *Nature Climate Change*, *9*(9), 684–689.  
469 <https://doi.org/10.1038/s41558-019-0545-2>
- 470 Thornton, P. E., Doney, S. C., Lindsay, K., Moore, J. K., Mahowald, N., Randerson, J. T., et al. (2009). Carbon-  
471 nitrogen interactions regulate climate-carbon cycle feedbacks: results from an atmosphere-ocean general  
472 circulation model. *Biogeosciences*, *6*(10), 2099–2120. <https://doi.org/10.5194/bg-6-2099-2009>
- 473 Versegny, D. L. (1991). CLASS — A Canadian land surface scheme for GCMS. I. Soil model. *International*  
474 *Journal of Climatology*, *11*(2), 111–133.
- 475 Versegny, D. L., McFarlane, N. A., & Lazare, M. (1993). CLASS — A Canadian land surface scheme for GCMS,  
476 II. Vegetation model and coupled runs. *International Journal of Climatology*, *13*(4), 347–370.  
477 <https://doi.org/10.1002/joc.3370130402>
- 478 Vitousek, P. M., Menge, D. N., Reed, S. C., & Cleveland, C. C. (2013). Biological nitrogen fixation: rates, patterns  
479 and ecological controls in terrestrial ecosystems. *Philosophical Transactions of the Royal Society B:*  
480 *Biological Sciences*, *368*(1621), 20130119–20130119. <https://doi.org/10.1098/rstb.2013.0119>

- 481 Walker, A. P., Kauwe, M. G. D., Bastos, A., Belmecheri, S., Georgiou, K., Keeling, R. F., et al. (2020). Integrating  
482 the evidence for a terrestrial carbon sink caused by increasing atmospheric CO<sub>2</sub>. *New Phytologist*, *229*(5),  
483 2413–2445. <https://doi.org/10.1111/nph.16866>
- 484 Wang, R., Goll, D., Balkanski, Y., Hauglustaine, D., Boucher, O., Ciais, P., et al. (2017). Global forest carbon  
485 uptake due to nitrogen and phosphorus deposition from 1850 to 2100. *Global Change Biology*, *23*(11),  
486 4854–4872. <https://doi.org/10.1111/gcb.13766>
- 487 Wang, S., Zhang, Y., Ju, W., Chen, J. M., Ciais, P., Cescatti, A., et al. (2020). Recent global decline of CO<sub>2</sub>  
488 fertilization effects on vegetation photosynthesis. *Science*, *370*(6522), 1295–1300.  
489 <https://doi.org/10.1126/science.abg4420>
- 490 Wang, Y. P., Zhang, Q., Pitman, A. J., & Dai, Y. (2015). Nitrogen and phosphorous limitation reduces the effects of  
491 land use change on land carbon uptake or emission. *Environmental Research Letters*, *10*(1).  
492 <https://doi.org/10.1088/1748-9326/10/1/014001>
- 493 Wang, Z., & Wang, C. (2021). Magnitude and mechanisms of nitrogen-mediated responses of tree biomass  
494 production to elevated CO<sub>2</sub>: A global synthesis. *Journal of Ecology*, *109*(12), 4038–4055.  
495 <https://doi.org/10.1111/1365-2745.13774>
- 496 Wieder, W. R., Cleveland, C. C., Smith, W. K., & Todd-Brown, K. (2015). Future productivity and carbon storage  
497 limited by terrestrial nutrient availability. *Nature Geoscience*, *8*(6), 441–444.  
498 <https://doi.org/10.1038/ngeo2413>
- 499 Wright, S. J., Turner, B. L., Yavitt, J. B., Harms, K. E., Kaspari, M., Tanner, E. V. J., et al. (2018). Plant responses  
500 to fertilization experiments in lowland, species-rich, tropical forests. *Ecology*, *99*(5), 1129–1138.  
501 <https://doi.org/10.1002/ecy.2193>
- 502 Zaehle, S., Friedlingstein, P., & Friend, A. D. (2010). Terrestrial nitrogen feedbacks may accelerate future climate  
503 change. *Geophysical Research Letters*, *37*(1). <https://doi.org/10.1029/2009GL041345>
- 504